The Application of Hypercomplex Matrix Analysis to Variable Parameter Networks*

S. KRONGELB†, MEMBER, IRE, J. J. McNICHOL†, MEMBER, IRE, AND N. KROLL‡

Summary—**The hypercomplex matrix methods developed to treat variable parameter elements are reviewed. The application of these techniques to the linear analysis of networks of variable parameter elements is demonstrated by considering a specific problem. A network containing two resonated variable capacitors separated by one-eighth wavelength of transmission line is first considered by the phase dependent admittance method. A partial treatment of the subharmonic case is given by this method to provide a physically plausible understanding of the network behavior. The complete problem is treated by the hypercomplex matrix methods. The discussion of the results illustrates how the network properties are determined from the mathematical formalism. Calculated characteristics of the two-capacitor network are given for several values of circuit parameters.**

I. Introduction

CIRCUITS CONTAINING time-varying elements are usually analyzed by representing the time-varying reactive components by phase dependent negative conductances. While adequate for simple circuits, this approach is not applicable to complicated networks because the phases at each component (and thus the corresponding negative conductances) are not known at the outset. In his treatment of traveling-wave amplifiers, Kroll[1] has shown how the phase dependent admittance can be written in a matrix form which is phase independent. If we combine the matrix admittance with the techniques of ordinary circuit theory, the result is a powerful tool for handling networks containing time-varying components. It is the purpose of this paper to review the matrix representation for variable parameter elements and to show, by application to a directional parametric amplifier, how this formalism is used in circuit analysis.

We will first require an understanding of the mathematical description of a variable capacitor,[2] and this is developed in Section II. We will show that a capacitor varied at angular frequency 2ω responds to a subharmonic voltage at angular frequency ω in a way which can be represented by a phase dependent admittance. Since phase dependent quantities are awkward to work with, we will, by suitably defining the voltage and current as vectors, write the admittance function as a matrix which does not involve the phase. The matrix will be expressed as a hypercomplex number, a form which proves convenient for circuit analysis since there is a correlation between the components of this representation and the real and imaginary parts of ordinary complex numbers. The hypercomplex admittance formulation can also be developed for the nonsubharmonic case. This extension to arbitrary frequencies will be made to give us a method for calculating the frequency response of networks.

When we have developed the hypercomplex admittance formalism, we will have sufficient background to analyze networks containing variable parameter elements. The use of these principles is best illustrated by applying them to a specific problem. We will, therefore, in Section III, introduce a network consisting of two resonated variable capacitors which are separated by one-eighth wavelength (at the signal frequency) of transmission line and which are driven by pump voltages which differ in phase by 90°. This network is of particular interest since it illustrates a means of obtaining directionality in parametric circuits.[3] The problem will first be treated in terms of the phase dependent admittance representation. Although this method is not too convenient mathematically, it has the advantage of providing a physical explanation for the circuit behavior which is obscured by the matrix formalism. The phase dependent admittance treatment will, therefore, make plausible the results of the matrix analysis.

In Sections IV and V we will respectively solve the subharmonic and arbitrary frequency cases using hypercomplex matrix analysis. The discussion will illustrate how the hypercomplex admittance developed in Section II is combined with the usual techniques of circuit analysis. We will set up the problem as if the network were an ordinary circuit and show how to substitute hypercomplex matrices for ordinary admittances and vectors for voltages and currents. Since we have replaced ordinary admittances by matrices, the problem becomes mathematically complicated. However, by properly interpreting the voltage vectors which represent the input and output, the solutions can be obtained in familiar terms. These solutions are discussed in Section VI.

* Received January 19, 1962; this work was supported in part by the Department of Defense under Contract No. NOBSR 63472.

† IBM Corporation, Thomas J. Watson Research Center, Yorktown Heights, N. Y.

‡ Department of Physics, University of California, La Jolla, Calif.; on leave from Columbia University, New York, N. Y.

[1] N. Kroll, "Properties of Propagating Structures with Variable Parameter Elements," presented at ONR Symposium on Microwave Techniques for Computers, Washington, D. C.; March 12, 1959.

[2] Throughout our discussion we shall assume the variable elements to be capacitors. The methods described, however, are applicable to any variable parameter component. In fact, the circuit chosen for illustration would work equally well with variable inductors.

[3] K. E. Schreiner, private communication, August 7, 1958.

II. Mathematical Background

As indicated in the Introduction, we begin by formulating the mathematical representation for variable parameter elements. The variable capacitor is here considered in the linear approximation, that is, the signal voltage is so much smaller than the pump voltage that we may neglect the capacitance variation caused by the signal. Further we assume that the capacitance variation is a linear function of the pump voltage so that the capacitance may be written as

$$C = C_0[1 + 2\rho \cos 2(\omega t + \psi)] \tag{1}$$

where 2ω is the angular frequency of the pump.

In any real parametric circuit the voltage sensitive capacitor has a capacitance-voltage function similar to that of Fig. 1. The pump is a sinusoidal voltage centered near the point $v = 0$. Thus (1) constitutes only the leading terms of a series representation for the true capacitance variation. In addition, anything except an infinitesimal signal will result in a capacitance variation beyond that caused by the pump. Our approximations are supported by the facts that 1) we can mathematically show that the higher terms in the capacitance series have a small effect and 2) laboratory work at least qualitatively substantiates predictions based on these approximations.

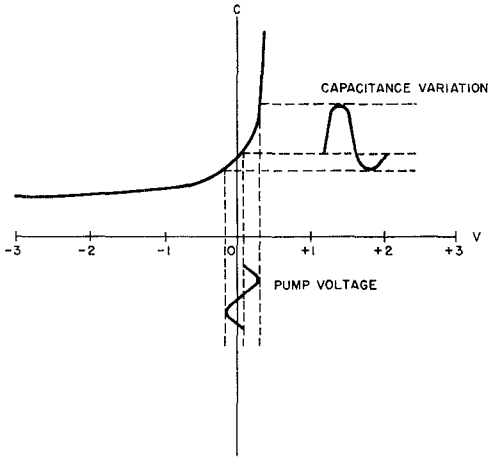

Fig. 1—Capacitance variation resulting from sinusoidal pump voltage applied to typical variable capacitor.

Phase Dependent Admittance

Within the framework of the approximations just discussed, the properties of a variable capacitor for a signal at one-half the pump frequency can be expressed by an admittance function. Just as for an ordinary capacitor, we start with the relation

$$q = Cv$$

where v is the signal voltage. The current through the capacitor is the time derivative of the charge so that, if we write $v = V_0 \cos(\omega t + \phi)$ and use (1) for C, we readily obtain (neglecting the current component at 3ω)

$$i = \frac{dq}{dt} = -\omega C_0[1 + \rho \cos 2(\phi - \psi)]V_0 \sin(\omega t + \phi) + \rho\omega C_0 \sin 2(\phi - \psi)V_0 \cos(\omega t + \phi). \tag{2}$$

From this expression we see that the admittance is

$$Y = j\omega C_0[1 + \rho \cos 2(\phi - \psi)] + \rho\omega C_0 \sin 2(\phi - \psi) \tag{3}$$

where $j = \sqrt{-1}$.

Thus far we have proceeded exactly as one does in setting up the admittance for ordinary ac components. The effect of pumping the capacitor manifests itself in our admittance function in two ways: 1) the admittance expression contains a conductive term, and 2) both the conductance and susceptance depend on the relative phase of the signal and pump. The fact that certain values of phase make the conductance negative indicates that the variable capacitor may be used as an amplifier or oscillator.

The Matrix Admittance

The admittance we have derived expresses the properties of a variable capacitor but is awkward to apply to any but the simplest networks because the admittance is a function of the phase of the voltage. To derive a phase independent admittance, we express our voltage as

$$v = v_1 \cos \omega t - v_2 \sin \omega t$$

where $v_1 = V_0 \cos \phi$ and $v_2 = V_0 \sin \phi$. We can also write this voltage as a mathematical vector

$$\boldsymbol{v} = \begin{pmatrix} v_1 \\ v_2 \end{pmatrix}.$$

Similarly, the current can be written as

$$\boldsymbol{i} = \begin{pmatrix} i_1 \\ i_2 \end{pmatrix}.$$

We can now define an admittance matrix relating the voltage and current in this new representation. It is simple to verify that the expression

$$\boldsymbol{i} = \overline{Y}\boldsymbol{v} \tag{4}$$

with the admittance matrix $\overline{Y}$ given by

$$\overline{Y} = \omega C_0 \begin{pmatrix} -\rho \sin 2\psi & -1 + \rho \cos 2\psi \\ 1 + \rho \cos 2\psi & \rho \sin 2\psi \end{pmatrix} \tag{5}$$

is equivalent to (2).

Voltage and current vectors and matrix admittances and impedances are used in circuit analysis in the same way that we use the complex quantities of ordinary ac analysis. All the methods of circuit analysis are applicable if we formally substitute vectors for the voltages and currents and matrices for the admittances

and impedances. The principle of using matrices and vectors in circuit analysis is best illustrated by application to a specific problem, and the succeeding sections are devoted to such an example. First, however, let us consider some properties of the admittance matrix which will simplify its use and show a correlation to the real and imaginary parts of complex admittances.

The Hypercomplex Representation

Any 2×2 matrix can be written as a linear combination of certain unit matrices. (Such a breakdown is analogous to writing a position vector in terms of unit vectors along the x, y, and z axes.) The system of unit matrices is

$$\hat{1} = \begin{pmatrix} 1 & 0 \\ 0 & 1 \end{pmatrix} \hat{\jmath} = \begin{pmatrix} 0 & -1 \\ 1 & 0 \end{pmatrix} \hat{k} = \begin{pmatrix} 1 & 0 \\ 0 & -1 \end{pmatrix} \hat{l} = \begin{pmatrix} 0 & 1 \\ 1 & 0 \end{pmatrix}$$

and any matrix $\overline{M}$ may be written as a linear combination

$$\overline{M} = \alpha\hat{1} + \beta\hat{\jmath} + \gamma\hat{k} + \delta\hat{l}.$$

$\overline{M}$ as thus written is called a hypercomplex number. Certain properties of the unit matrices which are useful and may be readily verified are:

$$\begin{aligned} \hat{\jmath}^2 &= -\hat{1} \qquad \hat{k}^2 = \hat{l} = \hat{1} \\ \hat{\jmath}\hat{k} &= -\hat{k}\hat{\jmath} = \hat{l} \\ \hat{l}\hat{\jmath} &= -\hat{\jmath}\hat{l} = \hat{k} \\ \hat{l}\hat{k} &= -\hat{k}\hat{l} = \hat{\jmath}. \end{aligned}$$

It is also useful to note that Euler's theorem $e^{\hat{\jmath}\rho} = \cos\theta + \hat{\jmath}\sin\theta$ holds in hypercomplex form.

The advantage of the hypercomplex representation becomes apparent when we apply it to the matrix admittance of (5). In hypercomplex form this admittance is

$$\begin{aligned} \overline{Y} &= \hat{\jmath}\omega C_0 + \rho\omega C_0(\hat{l}\cos 2\psi - \hat{k}\sin 2\psi) \\ &= \hat{\jmath}\omega C_0 + \rho\omega C_0\hat{l}e^{-2\hat{\jmath}\psi} \\ &= e^{\hat{\jmath}\psi}\hat{\jmath}\omega C_0(\hat{1} + \hat{k}\rho)e^{-\hat{\jmath}\psi}. \end{aligned} \tag{6}$$

The correlation between hypercomplex admittances and the usual complex admittances now becomes apparent. If we set $\rho = 0$ in the above expressions, we get the hypercomplex admittance for an ordinary capacitor as $\overline{Y} = \hat{\jmath}\omega C_0$. This formula is similar to the complex admittance except that $j = \sqrt{-1}$ is replaced by

$$= \begin{pmatrix} 0 & -1 \\ 1 & 0 \end{pmatrix}.$$

The correspondence of $\jmath$ to $\hat{\jmath}$ is carried even further when we note that $\hat{\jmath}\hat{\jmath} = -\hat{1}$. In general, we can write hypercomplex admittances and impedances from complex admittances and impedances by using the real part as the coefficient of $\hat{1}$ and the imaginary part as the coefficient of $\hat{\jmath}$. Thus, in the hypercomplex representation, the impedance of a resistor and inductor would be, respectively, $\overline{Z}_R = R\hat{1}$ and $\overline{Z}_L = \hat{\jmath}\omega L$.[4]

Arbitrary Frequency Case

Our treatment thus far has been restricted to a signal frequency of exactly half the pump frequency. If a signal with frequency not equal to half the pump frequency is fed into a parametric circuit, then the output will contain both the original frequency and an idler frequency. This fact can be mathematically represented by the equations

$$\begin{aligned} I(\omega_1) &= \overline{Y}_{11}V(\omega_1) + \overline{Y}_{12}\hat{k}V(\omega_2) \\ I(\omega_2) &= \overline{Y}_{21}\hat{k}V(\omega_1) + \overline{Y}_{22}V(\omega_2) \end{aligned} \tag{7}$$

where the currents and voltages are considered to be vectors as in the preceding paragraphs.

Eq. (7) is convenient if there is a real distinction between signal and idler as, for instance, would be the case if the signal and idler were well separated from each other so that the idler could be excluded from the output by means of a filter. For circuits operating near the subharmonic frequency, it is preferable to use a specialized form of signal. Let us consider a modulated signal where the carrier is exactly the subharmonic frequency and the angular modulation frequency is ν. Then the signal contains the angular frequencies $\omega_1 = \omega - \nu$ and $\omega_2 = \omega + \nu$ where $\omega = \omega_{\text{pump}/2}$. (We assume that the carrier amplitude is zero. If this is not so, the carrier can be handled separately by the analysis developed for the subharmonic case.) Note that the idler frequency for the ω_1 component of the signal is ω_2 and vice versa. Thus, the output for an amplitude modulated subharmonic input will have the same upper and lower sideband frequencies as the input, and the parametric action will not introduce any new frequencies.

Eq. (7) may now be specialized to the amplitude modulated signal. In matrix form, (7) reads

$$\begin{pmatrix} I(\omega_1) \\ I(\omega_2) \end{pmatrix} = \begin{pmatrix} \overline{Y}_{11} & \overline{Y}_{12}\hat{k} \\ \overline{Y}_{21}\hat{k} & \overline{Y}_{22} \end{pmatrix} \begin{pmatrix} V(\omega_1) \\ V(\omega_2) \end{pmatrix}. \tag{8}$$

The four component vector

$$\begin{pmatrix} V(\omega_1) \\ V(\omega_2) \end{pmatrix}$$

corresponds to a voltage

$$\begin{aligned} V(t) = {} & V_{11}\cos\omega_1 t - V_{12}\sin\omega_1 t \\ & + V_{21}\cos\omega_2 t - V_{22}\sin\omega_2 t. \end{aligned} \tag{9}$$

For an amplitude modulated voltage it is more convenient to talk about the angular carrier frequency ω and angular modulation frequency ν than about upper

[4] For convenience, the unity matrix will not be explicitly written. Thus $\overline{Z} = R$ implies $\overline{Z} = R\hat{1}$.

and lower sideband frequencies. Eq. (9) may be rewritten in terms of ω and ν as

$$V(t) = \text{Real Part}\left\{V^{\sim}{}_1 e^{j\nu t}\cos\omega t - V^{\sim}{}_2 e^{j\nu t}\sin\omega t\right\} \quad (10)$$

where

$$V^{\sim}{}_1 = V_1' e^{j\phi_1}$$
$$V^{\sim}{}_2 = V_2' e^{j\phi_2}$$

and the correspondence to (9) is expressed by

$$V_1'\cos\phi_1 = V_{11} + V_{21} \qquad V_1'\sin\phi_1 = V_{22} - V_{12}$$
$$V_2'\cos\phi_2 = V_{12} + V_{22} \qquad V_2'\sin\phi_2 = V_{11} - V_{21}$$
$$\omega_1 = \omega - \nu \qquad \omega_2 = \omega + \nu$$

We may represent the voltage $V(t)$ by a vector

$$V^{\sim} = \begin{pmatrix} V^{\sim}{}_1 \\ V^{\sim}{}_2 \end{pmatrix}.$$

If we compare this vector representation with that used in (8), we note that we now have a complex two-component vector rather than a real four-component vector. The current may be similarly represented by a complex vector and we may write a matrix relation

$$I^{\sim} = \overline{Y}^{\sim} V^{\sim} \quad (11)$$

where $\overline{Y}^{\sim}$ is a complex 2×2 matrix. It may be shown that, in the terms of (8), that

$$\overline{Y}^{\sim} = \tfrac{1}{2}(\underline{Y}_{11} + \underline{Y}_{22}) + \tfrac{1}{2}(\underline{Y}_{12} + \underline{Y}_{21})\hat{k} + j\hat{j}\left[\tfrac{1}{2}(\underline{Y}_{11} - \underline{Y}_{22}) + \tfrac{1}{2}(\underline{Y}_{12} - \underline{Y}_{21})\hat{k}\right]. \quad (12)$$

Since $\overline{Y}^{\sim}$ is a complex 2×2 matrix, we have written it in the hypercomplex representation and refer to it as a "complex" hypercomplex number. For the particular case of a variable capacitor

$$\overline{Y}^{\sim} = e^{\hat{j}\psi}(\hat{j}\omega + \hat{j}\hat{1}\nu)C_0(\hat{1} + \hat{k}\rho)e^{-\hat{j}\psi}. \quad (13)$$

Note that for $\nu = 0$, this expression reduces to (6) which was derived for the subharmonic voltage. We can also show that the complex hypercomplex impedance of a variable inductor is

$$\overline{Z}^{\sim} = e^{\hat{j}\psi}(\hat{j}\omega + \hat{j}\hat{1}\nu)L_0(\hat{1} + \hat{k}\rho)e^{-\hat{j}\psi}. \quad (14)$$

III. Phase Dependent Admittance Solution

In the preceding section we have seen how a variable capacitor can be represented by a phase dependent admittance and by a matrix admittance. These concepts and the methods of applying them will be clarified if we consider a specific problem.

The Two-Capacitor Circuit

The network chosen for the illustration is shown in Fig. 2. C_1 and C_2 are variable capacitors placed across a transmission line at points one-eighth of the subharmonic wavelength apart. An inductor L is placed across each capacitor and is chosen to resonate out the nonvarying portion of the capacitance at angular subharmonic frequency ω. The capacitors C_1 and C_2 are physically identical but differ in the phase of their pumps. The pump at C_2 lags that at C_1 by 90° so that we may write

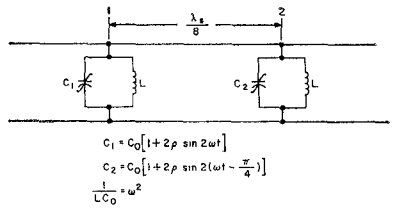

Fig. 2—Two-capacitor network used to illustrate mathematical formalism.

$$C_1 = C_0[1 + 2\rho\sin 2\omega t]$$

and

$$C_2 = C_0[1 + 2\rho\sin 2(\omega t - \pi/4)].$$

Because of the difference in pump phase between C_1 and C_2, the network looks different for a subharmonic signal traveling from right to left than it does for one going from left to right. Thus, we would expect the circuit to exhibit directionality. Also, as in any subharmonic parametric circuit, we would expect the behavior of the circuit to depend on the phase of the signal. In particular, we would like the network to amplify signals of a particular phase traveling from 1 to 2 and to attenuate those signals which are 90° different from the amplified phase. Also, we do not want amplification of signals of any phase traveling from 2 to 1.

The easiest way to analyze the circuit is by use of the matrix representation outlined in the preceding section. However, in formalizing the problem for mathematical convenience, the matrix method tends to obscure our physical feeling for the behavior of the circuit. Before proceeding with the matrix analysis, we shall, therefore, discuss the network in terms of phase dependent admittances. Because these admittances are of the same type we are familiar with for ordinary resistors and capacitors, the discussion should give us some physical understanding of the circuit.

Phase Dependent Admittance Analysis

The phase dependent admittance approach is to replace C_1 and C_2 by effective admittances (which of course, depend on the phase of the signal). A signal traveling along the transmission line will see these admittances as discontinuities which give rise to multiple reflections, the transmitted portions of which add up to the signal transmitted through the network.

In discussing the problem it is convenient to resolve the signal into two components separated in phase by 90°. One component, referred to as "in-phase," is of

the proper phase relative to the pump to make the conductance of the variable capacitor a negative maximum. The other component, called "out-of-phase" or "quadrature," then gives a maximum positive conductance. We shall only treat the case of an "in-phase" input at terminal 1 by the phase dependent admittance method and defer the complete solution to the more appropriate matrix analysis. The portion of the problem treated here should be sufficient to illustrate the phase dependent admittance and to provide an insight into the behavior of the network.

If we write the capacitance as

$$C = C_0[1 + 2\rho \sin 2(\omega t + \psi)]$$

and the signal voltage as $\sin(\omega t+\phi)$ then the phase dependent admittance is[5]

$$Y = -\rho\omega C_0 \cos 2(\phi - \psi) + j\omega C_0[1 + \rho \sin 2(\phi - \psi)]. \quad (15)$$

Since $\psi=0$ at C_1 the "in-phase" signal corresponds to $\phi=0$. The total admittance placed across the line at point 1 is obtained from (15) (and the fact that $j\omega C_0$ is resonated out by the inductance) as $G_x=-\rho\omega C_0$. This conductance represents a discontinuity on the transmission line. The effect of this discontinuity is to cause a reflection which, by ordinary transmission line theory, is characterized by a reflection coefficient

$$K = \frac{\dfrac{G_0}{G_P} - 1}{\dfrac{G_0}{G_P} + 1} \quad (16)$$

where G_0 is the characteristic admittance of the transmission line and $G_P=G_0+G_x$. We shall see that, for the case under discussion, only $G_x=\rho\omega C_0$ and $G_x=-\rho\omega C_0$ occur. Thus, it is convenient to set $r=|G_x/G_0|$ and to define

$$K_+ \equiv K(G_x > 0) = -\frac{r}{2 + r} \quad (17)$$

$$K_- \equiv K(G_x < 0) = \frac{r}{2 - r} \quad (18)$$

where the right-hand side of (17) and (18) follow directly from (16) and the definition of r. In this notation the reflection coefficient for the "in-phase" input wave at the first capacitor would be K_-.

We can now, with the aid of Fig. 3, follow the signal through its successive reflections. The portion of a unit incident wave which is transmitted past the first capacitor is (K_-+1). At the second capacitor this wave will still be "in-phase" with the pump at that point so that the reflection coefficient is again K_-. Thus, the part of

[5] Eq. (15) differs from (3) because of the different form assumed for the capacitance and signal voltage. If we substitute $\psi=\psi-45°$ and $\phi=\phi-90°$ for ψ and ϕ in (3), then we obtain (15).

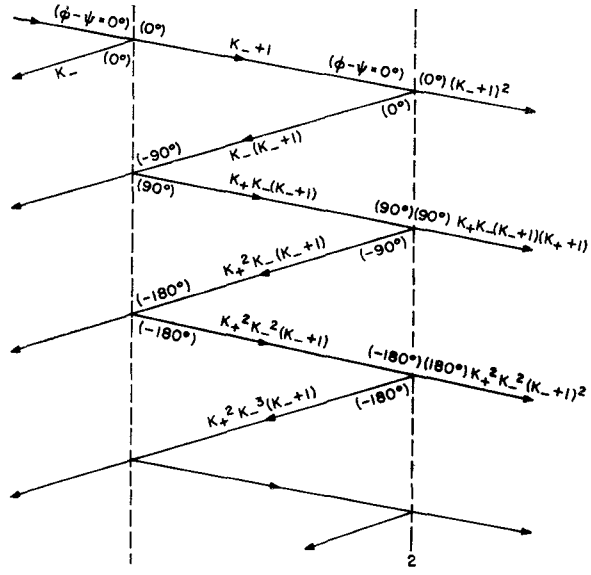

Fig. 3—Internal reflection path for an "in-phase" input to the network of Fig. 2.

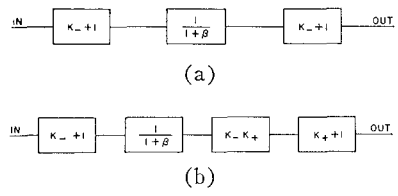

Fig. 4—Block diagram of feedback representation for "in-phase" input to two-capacitor network. (a) "In-phase" output. (b) "Out-of-phase" output.

the original signal which is transmitted past the second capacitance is $(K_-+1)^2$ while the part which is reflected back towards the input is $K_-(K_-+1)$.

When this reflected portion reaches the first capacitor, it will again be partially reflected. This time, however, the reflection coefficient will be K_+ since the signal has traversed the one-eighth wavelength section two times and thus lags the pump by 90°. The reflected signal is then given by $K_+K_-(K_-+1)$ and is shifted 180° in phase because it is reflected from a discontinuity whose impedance is less than the characteristic impedance of the line. Similar considerations give the amplitude after reflection by the second capacitor. By the time the signal gets back to the input it has made four traverses of the one-eighth wavelength section and has undergone two 180° phase changes at reflections. Thus, the next reflection is determined by K_- and we get a wave of amplitude $K_+^2K_-^2(K_-+1)$ which is 180° out of phase with the original input.

If we consider the component of the total output which is "in-phase" with the pump at the output, the network can be regarded as shown in Fig. 4(a). The blocks (K_-+1) represent the amplification by the variable capacitances. $1/(1+\beta)$ results from regarding the reflections as giving a feedback system in which a fraction $K_-^2K_+^2$ of the signal transmitted through the

transmission line section is fed back to the input. The over-all gain is readily found to be

$$A_{0^0} = (K_- + 1)^2 \frac{1}{1 + K_-^2 K_+^2}$$

$$= \frac{4(2 + r)}{(4 - r^2)^2 + r^4} . \tag{19}$$

If we consider the quadrature components of the output, it is not difficult to see that the network can be represented as in Fig. 4(b), and that the over-all gain for this portion of the output is

$$A_{90^0} = A_{0^0}\left(\frac{r}{2 + r}\right)^2 . \tag{20}$$

The feedback approach illustrates certain properties of the network. The blocks representing gain in Fig. 4 can be considered to arise from the negative conductance which an "in-phase" input signal sees the variable capacitor to be. Thus we would expect that an "out-of-phase" signal would see positive conductances and would be attenuated. Likewise, if a signal traveling in the reverse direction were "in-phase" at one capacitor, it would be "out-of-phase" at the other, and so there would be little, if any, over-all gain. We would also expect the forward gain to be increased by some attenuation between the capacitors. This paradoxical statement can be understood from the feedback approach when we remember that the portion of the signal which we regard as feedback has been reflected through the one-eighth wavelength section four times. Since the directly transmitted signal passes through only once, it is clear that attenuation would have a much stronger effect in reducing feedback than it would in attenuating the direct signal.

The properties we have just outlined are made plausible by the phase dependent admittance approach. We shall now verify them quantitatively by a hypercomplex matrix analysis of the problem.

IV. The Hypercomplex Treatment of Subharmonic Case

As indicated earlier, the hypercomplex analysis proceeds by using those techniques of ordinary circuit analysis which may be appropriate to the problem and formally substituting vectors for the currents and voltages, and matrices for the admittances and impedances. Since our problem can be considered as a cascading of a variable capacitor, a transmission line section, and another variable capacitor, the transmission matrix approach seems appropriate.[6]

The Ordinary Transmission Matrix

In the notation of Fig. 5 the transmission matrix

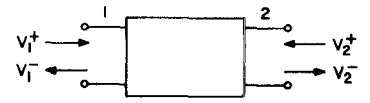

Fig. 5—Wave convention for transmission matrix.

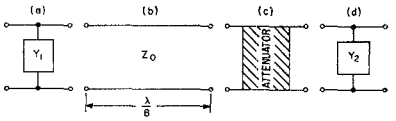

Fig. 6—Cascade equivalent of two-capacitor network.

equation is written as

$$\begin{pmatrix} V_2^- \\ V_2^+ \end{pmatrix} = \begin{pmatrix} T_{11} & T_{12} \\ T_{21} & T_{22} \end{pmatrix} \begin{pmatrix} V_1^+ \\ V_1^- \end{pmatrix} \tag{21}$$

where T_{ij} are the elements of the transmission matrix and the $(+)$ superscript indicates a wave incident on the network while a $(-)$ sign denotes an outgoing wave. In applying the transmission matrix to the variable capacitor problem, the voltages will be replaced by two component vectors so that the vectors in (21) will really have four components. Likewise, each of the T_{ij}'s will become 2×2 matrices.

The network of Fig. 2 may be regarded as a cascading of the sections shown in Fig. 6. Sections (a) and (d) are shunt elements C_1 and C_2 respectively, each in parallel with L. Section (b) is the one-eighth wavelength of transmission line while (c) represents an attenuation introduced between (a) and (d). We include the attenuator in our present treatment because our phase dependent admittance discussion has indicated that attenuation would have the interesting effect of increasing the gain.

The transmission matrix for the over-all network may now be determined by writing the matrices for each section and taking their product. Following Ramo and Whinnery,[7] the transmission matrices are:

$$\overline{T}_{(a)} = \begin{pmatrix} 1 - Z_0Y_1/2 & -Z_0Y_1/2 \\ Z_0Y_1/2 & 1 + Z_0Y_1/2 \end{pmatrix} \tag{22}$$

$$\overline{T}_{(d)} = \begin{pmatrix} 1 - Z_0Y_2/2 & -Z_0Y_2/2 \\ Z_0Y_2/2 & 1 + Z_0Y_2/2 \end{pmatrix} \tag{23}$$

$$\overline{T}_{(b)} = \begin{pmatrix} e^{-j\beta l} & 0 \\ 0 & e^{j\beta l} \end{pmatrix} = \frac{\sqrt{2}}{2}\begin{pmatrix} 1 - j & 0 \\ 0 & 1 + j \end{pmatrix} \tag{24}$$

$$T_{(c)} = \begin{pmatrix} \alpha & 0 \\ 0 & 1/\alpha \end{pmatrix}. \tag{25}$$

where α is a scalar attenuation factor defined by $V_2^- = \alpha V_1^+$ and $V_1^- = \alpha V_2^+$.

The transmission matrix for the whole network can now be obtained from the product of (22)–(25) as

$$\overline{T} = \overline{T}_{(d)}\overline{T}_{(c)}\overline{T}_{(b)}\overline{T}_{(a)}. \tag{26}$$

In performing the multiplication, we must be careful to

[6] See, for instance, S. Ramo and J. R. Whinnery, "Fields and Waves in Modern Radio," John Wiley and Sons, Inc., New York, N. Y.; pp. 461–463, 1953.

[7] Ramo and Whinnery, *op. cit.*, p. 463.

preserve the order of terms in the product since each of these terms will be replaced by a matrix. The evaluation of (26) is straightforward and, after some long algebra, we obtain

$$\overline{T} = \frac{\sqrt{2}}{2\alpha} \cdot \begin{pmatrix} \alpha^2(A-B)-C & \alpha^2(D-E)-(F+G+C) \\ \alpha^2(F-G)+(D+E+C) & A+B+C \end{pmatrix} \quad (27)$$

where

$$A = 1 + j\frac{Z_0Y_1}{2} + \frac{Z_0Y_2}{2}j$$

$$B = j + \frac{Z_0Y_1}{2} + \frac{Z_0Y_2}{2}$$

$$C = \frac{\beta^2Z_0^2Y_2Y_1}{4} + \frac{\gamma^2Z_0^2Y_2jY_1}{4}$$

$$D = Z_0jY_1/2 \qquad E = Z_0Y_1/2$$

$$F = Z_0Y_2/2 \qquad G = Z_0Y_2j/2$$

and

$$\beta^2 = 1 - \alpha^2 \qquad \gamma^2 = 1 + \alpha^2.$$

Hypercomplex Substitution

Thus far we have treated the problem exactly as if the network were made up of ordinary (nonvarying) components (except that we preserved the order of terms in the multiplication). We can now adapt this treatment to the variable capacitor problem by formally substituting the matrix $\hat{\jmath}$ for j and writing the admittances Y_1 and Y_2 in appropriate matrix form.[8] The admittance Y_1 for section (a) arises from the parallel combination of L and C_1. By (6) the matrix admittance would be

$$\overline{Y}_1 = \overline{Y}_L + \overline{Y}_{C_1} = -\frac{\hat{\jmath}}{\omega L} + \hat{\jmath}\omega C_0 + \rho\omega C_0\hat{l}e^{\hat{\imath}\pi/2}$$

where we have taken $\psi = -45°$. (See Footnote 5.) Because of resonance, the first two terms of $\overline{Y}_1$ cancel; the last term simplifies by Euler's theorem and we get

$$\overline{Y}_1 = \rho\omega C_0\hat{k}. \quad (28)$$

In similar fashion we get for Y_2 (with $\psi = -90°$)

$$\overline{Y}_2 = -\rho\omega C_0\hat{l}. \quad (29)$$

If we introduce $r = \rho\omega C_0Z_0$ and denote the elements of (27) by subscripts as in (21), the transcription of the $\overline{T}$ matrix to hypercomplex form yields

$$\overline{T}_{11} = \frac{\sqrt{2}}{4\alpha}\left[2\alpha^2 + \frac{\gamma^2}{2}r^2 + \hat{\jmath}\left(\frac{\beta^2}{2}r^2 - 2\alpha^2\right) + 2\alpha^2r\hat{l} - 2\alpha^2r\hat{k}\right]$$

$$\overline{T}_{12} = \frac{\sqrt{2}}{4\alpha}\left[\frac{\gamma^2}{2}r^2 + \frac{\beta^2}{2}r^2\hat{\jmath} + \gamma^2r\hat{l} + \beta^2r\hat{k}\right]$$

$$\overline{T}_{21} = \frac{\sqrt{2}}{4\alpha}\left[\frac{-\gamma^2}{2}r^2 - \frac{\beta^2}{2}r^2\hat{\jmath} + r\beta^2\hat{l} + r\gamma^2\hat{k}\right]$$

$$\overline{T}_{22} = \frac{\sqrt{2}}{4\alpha}\left[2 - \frac{\gamma^2}{2}r^2 + \hat{\jmath}\left(2 - \frac{\beta^2}{2}r^2\right)\right]. \quad (30)$$

Since each element written in (30) is a 2×2 matrix, the $\overline{T}$ matrix can be written as a 4×4 matrix with scalar elements. In this form

$$\overline{T} = \frac{\sqrt{2}}{4\alpha}\left[\begin{array}{c|c|c|c} 2\alpha^2 + \frac{\gamma^2}{2}r^2 - 2\alpha^2r^2 & 2\alpha^2r + 2\alpha^2 - \frac{\beta^2}{2}r^2 & \frac{\gamma^2}{2}r^2 + \beta^2r & \gamma^2r - \frac{\beta^2}{2}r^2 \\ \hline 2\alpha^2r - 2\alpha^2 + \frac{\beta^2}{2}r^2 & 2\alpha^2 + \frac{\gamma^2}{2}r^2 + 2\alpha^2r & \gamma^2r + \frac{\beta^2}{2}r^2 & \frac{\gamma^2}{2}r^2 - \beta^2r \\ \hline -\frac{\gamma^2}{2}r^2 + \gamma^2r & \beta^2r + \frac{\beta^2}{2}r^2 & 2 - \frac{\gamma^2}{2}r^2 & \frac{\beta^2}{2}r^2 - 2 \\ \hline \beta^2r - \frac{\beta^2}{2}r^2 & -\frac{\gamma^2}{2}r^2 - \gamma^2r & -\frac{\beta^2}{2}r^2 + 2 & 2 - \frac{\gamma^2}{2}r^2 \end{array}\right]. \quad (31)$$

The matrix of (31) combined with (21) completely represents the network if we write each of the voltage waves as a vector. We shall begin our solution by considering the same case as was treated by the phase dependent admittance method. In this way we can develop an understanding of the vector voltages.

[8] Rigorously, we should replace all admittances and impedances by matrices. However, Z_0 is a real impedance so that it would be replaced by the diagonal matrix

$$Z_0 = \begin{pmatrix} Z_0 & 0 \\ 0 & Z_0 \end{pmatrix} = Z_0 1.$$

Thus the term $Z_0\overline{Y}_1$, for instance, is equivalent to $\overline{Z_0Y_1}$ and so we retain Z_0 as a scalar.

TABLE I

NETWORK RESPONSE TO UNIT INPUT IN TERMS OF "IN-PHASE" AND "OUT-OF-PHASE" COMPONENTS

Output \ Input	In-Phase at Terminal 1	Out-of-Phase at Terminal 1	In-Phase at Terminal 2	Out-of-Phase at Terminal 2
Transmitted-in-Phase	$\frac{2\alpha(r+2)^2}{\delta}$	$\frac{-2\alpha^3r^2}{\delta}$	$\frac{-2\alpha^3r^2}{\delta}$	$\frac{2\alpha(4-r^2)}{\delta}$
Transmitted Out-of-Phase	$\frac{2\alpha^3r^2}{\delta}$	$\frac{2\alpha(2-r)^2}{\delta}$	$\frac{-2\alpha(4-r^2)}{\delta}$	$\frac{-2\alpha^3r^2}{\delta}$
Reflected in-Phase	$\frac{r(r+2)(2-\mu r^2)}{\delta}$	$\frac{-2\alpha^2r(2-r)}{\delta}$	$\frac{r(r+2)(2-\mu r^2)}{\delta}$	$\frac{2\alpha^2r(r+2)}{\delta}$
Reflected Out-of-Phase	$\frac{-2\alpha^2r(r+2)}{\delta}$	$\frac{-r(2-r)(2-\mu r^2)}{\delta}$	$\frac{2\alpha^2r(2-r)}{\delta}$	$\frac{-r(2-r)(2-\mu r^2)}{\delta}$

$$\delta = \mu r^4 - 4r^2 + 8 = \left(2 - \frac{\gamma^2}{2}r^2\right)^2 + \left(2 - \frac{\beta^2}{2}r^2\right)^2$$

$$\mu = \frac{1+\alpha^4}{2}$$

$$\beta^2 = 1 - \alpha^2$$

$$\gamma^2 = 1 + \alpha^2$$

Vector Representation of Inputs

The problem we treated by the phase dependent admittance was that of "in-phase" input $v = \sin \omega t$ at the left hand terminals of the network. According to our vector definition in Section II, an "in-phase" wave incident on the left corresponds to

$$\boldsymbol{V}_1^+ = \begin{pmatrix} 0 \\ -1 \end{pmatrix}. \tag{32a}$$

Since there is no input on the right (we assume a matched termination),

$$\boldsymbol{V}_2^+ = \begin{pmatrix} 0 \\ 0 \end{pmatrix}. \tag{32b}$$

The remaining quantities $\boldsymbol{V}_1^-$ and $\boldsymbol{V}_2^-$ represent, respectively, the reflected and transmitted portions of the signal to be determined.

In our phase dependent admittance treatment we determined only V_2^-, the transmitted output. In that discussion we resolved the output into a component which was "in-phase" with the pump at the output, and a component which was in quadrature. This resolution is a convenient one for a traveling pump and signal, and we shall retain it in our present discussion. Writing the output in this way corresponds to writing v as $A \cos(\omega t - \pi/4) - B \sin(\omega t - \pi/4)$ where $-B$ is the "in-phase" component and A the "out-of-phase." Since $\boldsymbol{V}_2^-$ is defined from $V_2^- = a \cos \omega t - b \sin \omega t$, we can obtain A and B from V_2^- by simple trigonometric manipulation. The expressions for A and $-B$ obtained by the matrix method (the actual solutions are given in Table I) are the same as (20) and (19), respectively.

The advantage of the matrix method arises from the fact that all aspects of the problem can be determined from the one matrix of (31). By the phase dependent admittance method we would have to repeat the entire problem from the beginning each time we changed the phase or position of the input. Using the matrix method, however, we write the appropriate vector for each input condition and solve the resulting equation. The problem is completely solved if in addition to (32), we consider the following three inputs:

An "out-of-phase" input on the left and no input on the right, represented by

$$\boldsymbol{V}_1^+ = \begin{pmatrix} 1 \\ 0 \end{pmatrix} \qquad \boldsymbol{V}_2^+ = \begin{pmatrix} 0 \\ 0 \end{pmatrix}. \tag{33}$$

An "in-phase" input at the right and no input on the left, represented by

$$\boldsymbol{V}_2^+ = -\frac{1}{\sqrt{2}}\begin{pmatrix} 1 \\ 1 \end{pmatrix} \qquad \boldsymbol{V}_1^+ = \begin{pmatrix} 0 \\ 0 \end{pmatrix}. \tag{34}$$

An "out-of-phase" input at the right and no input on the left, represented by

$$\boldsymbol{V}_2^+ = \frac{1}{\sqrt{2}}\begin{pmatrix} 1 \\ -1 \end{pmatrix} \qquad \boldsymbol{V}_1^+ = \begin{pmatrix} 0 \\ 0 \end{pmatrix}. \tag{35}$$

For each of these inputs there will be a transmitted wave on the side of the network opposite the nonzero input and a reflected wave on the same side as the input. Each of these outputs is resolved into an "in-phase" and an "out-of-phase" component and the gain (output/input) for each component is tabulated in Table I. The outputs may also be expressed in terms of amplitude and phase shift; this representation is given in Table II for the four input conditions.

TABLE II

NETWORK RESPONSE TO UNIT INPUT IN TERMS OF AMPLITUDE AND PHASE SHIFT

Output \ Input	In-Phase at Terminal 1	Out-of-Phase at Terminal 1	In-Phase at Terminal 2	Out-of-Phase at Terminal 2
Transmitted Amplitude	$\frac{2\alpha}{\delta}[\alpha^4r^4+(r+2)^4]^{1/2}$	$\frac{2\alpha}{\delta}[\alpha^4r^4+(2-r)^4]^{1/2}$	$\frac{2\alpha}{\delta}[\alpha^4r^4+(4-r^2)^2]^{1/2}$	$\frac{2\alpha}{\delta}[(4-r^2)^2+\alpha^4r^4]^{1/2}$
Transmitted Phase	$\tan^{-1}\left[\frac{\alpha^2r^2-(r+2)^2}{\alpha^2r^2+(r+2)^2}\right]$	$\tan^{-1}\left[\frac{\alpha^2r^2-(2-r)^2}{\alpha^2r^2+(2-r)^2}\right]$	$\tan^{-1}\left[\frac{(1-\alpha^2)r^2-4}{4-(1+\alpha^2)r^2}\right]$	$\tan^{-1}\left[\frac{(1-\alpha^2)r^2-4}{-(\alpha^2+1)r^2+4}\right]$
Reflected Amplitude	$\frac{r(r+2)}{\delta}[(2-\mu r^2)^2+4\alpha^4]^{1/2}$	$\frac{r(2-r)}{\delta}[(2-\mu r^2)^2+4\alpha^4]^{1/2}$	$\frac{r}{\delta}[(r+2)^2(2-\mu r^2)^2+4\alpha^4(2-r^2)]^{1/2}$	$\frac{r}{\delta}[(2-r)^2(2-\mu r^2)^2+4\alpha^4(r+2^2]^{1/2}$
Reflected Phase	$\tan^{-1}\left[\frac{-2\alpha^2}{2-\mu r^2}\right]$	$\tan^{-1}\left[\frac{2\alpha^2(2-r)}{-(2-r)(2-\mu r^2)}\right]$	$\tan^{-1}\left[\frac{2\alpha^2(2-r)}{(r+2)(2-\mu r^2)}\right]$	$\tan^{-1}\left[\frac{-2\alpha^2(r+2)}{-(2-r)(2-\mu r^2)}\right]$

(The ambiguity in phase angle (ϕ) is removed by the rule that $\sin\phi$ has the same sign as the numerator of the algebraic expression for $\tan\phi$.)

V. BANDWIDTH ANALYSIS

The question which arises in the practical application of any circuit is "What is the bandwidth?" We shall now consider this problem for our two-capacitor network, thereby illustrating the complex hypercomplex formalism developed for bandwidth analysis. The transmission matrix approach is applicable to the bandwidth problem if we use the complex hypercomplex admittances rather than the hypercomplex form used in the subharmonic treatment. (The pure subharmonic solution can, in fact, be obtained from the bandwidth analysis. The reader, however, should profit from seeing the conceptually simpler real hypercomplex analysis applied separately and can now follow the present treatment with an eye towards seeing how it reduces to our earlier work.)

Complex Hypercomplex Transmission Matrix

The complex hypercomplex formalism was developed to specifically treat the case of a subharmonic carrier ω amplitude modulated at angular frequency ν. If we write this signal as in (10)

$$V(t) = \text{Real Part}\left\{V\tilde{}_1 e^{j\nu t}\cos\omega t - V\tilde{}_2 e^{j\nu t}\sin\omega t\right\} \quad (36)$$

then we could define a complex vector representation

$$V\tilde{} = \begin{pmatrix} V\tilde{}_1 \\ V\tilde{}_2 \end{pmatrix}.$$

A complex hypercomplex admittance relating this voltage vector to the current written in the same form was defined by (11) and was stated for a variable capacitor in (13). If we write the transmission matrix of (21) with complex hypercomplex elements and express the voltage waves as complex vectors, we can obtain the solution to our bandwidth problem. The transmission matrix will be a function of the angular modulation frequency ν so we can determine the output waves as a function of ν for any particular input.

Just as in the subharmonic case, we obtain the transmission matrix by considering the cascaded sections of Fig. 6 so that $\overline{T}$, as in (26) is

$$\overline{T} = \overline{T}_{(d)}\overline{T}_{(c)}\overline{T}_{(b)}\overline{T}_{(a)}.$$

$\overline{T}_{(a)}$ and $\overline{T}_{(d)}$ are the same as (22) and (23) where now Y_1 and Y_2 will be complex hypercomplex numbers. Y_1 is the admittance of the parallel combination C_1 and L so that

$$\overline{Y}\tilde{}_1 = (\overline{Y}\tilde{})_{C_1} + (\overline{Y}\tilde{})_L. \quad (37)$$

$(\overline{Y}\tilde{})_{C_1}$ is obtained from (13) by setting $\psi = -45°$ (see Footnote 5) as

$$(\overline{Y}\tilde{})_{C_1} = [jqf + \hat{\jmath}q - jrf\hat{l} + r\hat{k}]Z_0^{-1}. \quad (38)$$

We have introduced here, in addition to the abbreviation $r = \rho\omega C_0 Z_0$, the notation

$$f = \nu/\omega$$

and

$$q = \omega C_0 Z_0.$$

The complex hypercomplex admittance of the inductance is obtained from (14) with $\rho = 0$ so that, neglecting quadratic and higher terms in f,

$$(\overline{Y}\tilde{})_L = (\overline{Z}\tilde{})_L^{-1} \approx -\frac{\hat{\jmath}}{\omega L} + j\frac{f}{\omega L}. \quad (39)$$

$\overline{Y}\tilde{}_1$ is obtained by substituting (38) and (39) into (37) and using the resonance condition $\omega C_0 = 1/\omega L$ to get

$$\overline{Y}\tilde{}_1 = [2jqf - jrf\hat{l} + r\hat{k}]Z_0^{-1}. \quad (40)$$

In similar fashion we find

$$\overline{Y}\tilde{}_2 = [2jqf - jrf\hat{k} - r\hat{l}]Z_0^{-1}. \quad (41)$$

Eqs. (40) and (41), when substituted in (22) and (23), determine $\overline{T}\tilde{}_{(a)}$ and $\overline{T}\tilde{}_{(d)}$. (We may note that

(40) and (41) reduce to (28) and (29) respectively at $f=0$.) The resulting matrices in their 4×4 forms are

$$\overline{T}^{\sim}_{(a)} = \frac{1}{2}\left[\begin{array}{c|c|c|c} 2-r-j2qf & jrf & -r-j2qf & jrf \\ \hline jrf & 2+r-j2qf & jrf & r-j2qf \\ \hline r+j2qf & -jrf & 2+r+j2qf & -jrf \\ \hline -jrf & -r+j2qf & -jrf & 2-r+j2qf \end{array}\right] \tag{42}$$

and

$$\overline{T}^{\sim}_{(d)} = \frac{2}{2}\left[\begin{array}{c|c|c|c} 2+j(-2qf+rf) & r & j(-2qf+rf) & r \\ \hline r & 2-j(2qf+rf) & r & -j(2qf+rf) \\ \hline j(2qf-rf) & -r & 2+j(2qf-rf) & -r \\ \hline -r & j(2qf+rf) & -r & 2+j(2qf+rf) \end{array}\right]. \tag{43}$$

We can also show that

$$\overline{T}^{\sim}_{(c)}\overline{T}^{\sim}_{(b)} = \frac{\sqrt{2}}{2\alpha}\left[\begin{array}{c|c|c|c} \alpha^2 e^{-jf\pi/4} & \alpha^2 e^{-jf\pi/4} & 0 & 0 \\ \hline -\alpha^2 e^{-jf\pi/4} & \alpha^2 e^{-jf\pi/4} & 0 & 0 \\ \hline 0 & 0 & e^{jf\pi/4} & -e^{jf\pi/4} \\ \hline 0 & 0 & e^{jf\pi/4} & e^{jf\pi/4} \end{array}\right]. \tag{44}$$

The matrices of (42)–(44) are rather complicated. Their product, which is the transmission matrix for the entire network, would be even more intractable, and we would not readily see the properties of the network from this complicated matrix. It, therefore, seems best to continue the problem numerically with the aid of a computer. The computer (an IBM 704) is programmed to receive the matrices of (42)–(44) in numerical form and to manipulate them so that the properties of the network can be read directly from the computer output.

We ask the computer to determine a scattering matrix from the over-all transmission matrix. Transmission matrices are convenient for setting up the problem initially since the over-all matrix is the product of the matrices for the individual sections. However, the transmission matrix does not conveniently relate output voltages to the input. For instance, in the subharmonic problem we had to solve a system of simultaneous equations to get our solution.

The scattering matrix, on the other hand, expresses output quantities in terms of input and is defined by

$$\begin{pmatrix} V_{(2)}^{-} \\ V_{(1)}^{-} \end{pmatrix} = \overline{T}' \begin{pmatrix} V_{(1)}^{+} \\ V_{(2)}^{+} \end{pmatrix}. \tag{45}$$

Eq. (45) is seen to be a rearrangement of (21) with outgoing waves (negative superscripts) on the left. Our solution is thus determined from the input by the multiplication of a simple vector by a matrix which is obtained from the transmission matrix by a transformation which is programmed into the computer.[9] [We note that (45) differs from the usual scattering matrix definition in that $V_{(2)}^{-}$ and $V_{(1)}^{-}$ are interchanged.)

[9] When we solved the simultaneous equations which arose in treating the subharmonic case we, in effect, determined $\overline{T}'$. The solution of simultaneous equations can be expressed mathematically as a matrix transformation. The equations which arose in the subharmonic case were so simple, however, that it was not necessary to introduce the mathematical sophistication of a matrix transformation.

Input Vectors

Thus far we have seen how to determine our solution in terms of a vector representation. It remains for us now to specify our input waves in vector form and to see how to interpret the output vectors as ordinary voltages. Our input wave consists of an amplitude-modulated subharmonic carrier and may be written as

$$v = \sin(\omega t + \phi)\cos \nu t.$$

Just as for the unmodulated input, it seems reasonable that maximum gain would occur when the carrier of a signal incident from the left in Fig. 2 was "in-phase" with the pump at the first capacitor; *i.e.*, $\phi = 0$. We therefore want to express the voltage wave

$$V_{(1)}{}^{+}(t) = \sin \omega t \cos \nu t. \tag{46}$$

As may be seen by use of (36), the vector representation for this "in-phase" input is

$$\tilde{V}_1{}^{+} = \begin{pmatrix} 0 \\ -1 \end{pmatrix}. \tag{47}$$

In this manner we can determine the vector representation for any carrier phase. As for the subharmonic problem, the four cases specified in (32)–(35) are of interest here. These input conditions and their vector representations are:

a) "In-phase" carrier at left and no input on right

$$\tilde{V}_1{}^{+} = \begin{pmatrix} 0 \\ -1 \end{pmatrix} \qquad \tilde{V}_2{}^{+} = \begin{pmatrix} 0 \\ 0 \end{pmatrix} \tag{48}$$

b) "Out-of-phase" carrier at left and no input at right

$$\tilde{V}_1{}^{+} = \begin{pmatrix} 1 \\ 0 \end{pmatrix} \qquad \tilde{V}_2{}^{+} = \begin{pmatrix} 0 \\ 0 \end{pmatrix} \tag{49}$$

c) "In-phase" carrier at the right and no input at left

$$\tilde{V}_2{}^{+} = -\frac{1}{\sqrt{2}}\begin{pmatrix} 1 \\ 1 \end{pmatrix} \qquad \tilde{V}_1{}^{+} = \begin{pmatrix} 0 \\ 0 \end{pmatrix} \tag{50}$$

d) "Out-of-phase" carrier at right and no input at left

$$\tilde{V}_2{}^{+} = \frac{1}{\sqrt{2}}\begin{pmatrix} 1 \\ -1 \end{pmatrix} \qquad \tilde{V}_1{}^{+} = \begin{pmatrix} 0 \\ 0 \end{pmatrix}. \tag{51}$$

Output Vectors and Their Interpretation

The output waves $V_{(1)}{}^{-}$ and $V_{(2)}{}^{-}$ may now be determined for each of the input conditions by substitution into (45). We shall consider the details only for the input of (48). Eq. (45) combined with (48) reads

$$\begin{pmatrix} \tilde{V}_2{}^{-} \\ \tilde{V}_1{}^{-} \end{pmatrix} = \begin{vmatrix} \tilde{t}_{11} & \tilde{t}_{12} & \tilde{t}_{13} & \tilde{t}_{14} \\ \tilde{t}_{21} & \tilde{t}_{22} & \tilde{t}_{23} & \tilde{t}_{24} \\ \tilde{t}_{31} & \tilde{t}_{32} & \tilde{t}_{33} & \tilde{t}_{34} \\ \tilde{t}_{41} & \tilde{t}_{42} & \tilde{t}_{43} & \tilde{t}_{44} \end{vmatrix} \begin{vmatrix} 0 \\ -1 \\ 0 \\ 0 \end{vmatrix} \tag{52}$$

where we assume that the individual elements of the $\bar{T}'$ matrix have been calculated. $\tilde{V}_2{}^{-}$ is then easily seen to be

$$\tilde{V}_2{}^{-} = \begin{pmatrix} -\tilde{t}_{12} \\ -\tilde{t}_{22} \end{pmatrix}.$$

From our definition of (36) we may write

$$\begin{aligned} V_2{}^{-}(t) &= \text{Real Part}\left\{-\tilde{t}_{12}e^{j\nu t}\cos \omega t + \tilde{t}_{22}e^{j\nu t}\sin \omega t\right\} \\ &= \text{Real Part}\left\{\tfrac{1}{2}(-\tilde{t}_{12} - j\tilde{t}_{22})e^{j(\omega+\nu)t} \right. \\ &\qquad \left. + \tfrac{1}{2}(-\tilde{t}_{12} + j\tilde{t}_{22})e^{-j(\omega-\nu)t}\right\} \end{aligned} \tag{53}$$

where the second line is obtained from the first by trigonometric manipulation. The $(\omega+\nu)$ component of the output (upper sideband) is thus determined by the quantity

$$\tilde{t}_{\omega+\nu} = -\tfrac{1}{2}(\tilde{t}_{12} + j\tilde{t}_{22}). \tag{54}$$

The $(\omega-\nu)$ component, or lower sideband, is conveniently stated as the complex conjugate of these elements. By taking the complex conjugate of the brackets in (53), it follows that the $(\omega-\nu)$ component is determined by

$$\tilde{t}_{\omega-\nu} = -\tfrac{1}{2}(\tilde{t}_{12}{}^{*} + j\tilde{t}_{22}{}^{*}). \tag{55}$$

We have shown so far that for an amplitude modulated input of the form $(\sin \omega t \cos \nu t)$ as in (46) the upper and lower sidebands of the output are given by (54) and (55), respectively. It is usual to express the relation between input and output in terms of an amplitude change (or gain) and phase shift. Since the input of (46) can be written as

$$V_1{}^{+}(t) = \tfrac{1}{2}[\sin(\omega + \nu)t + \sin(\omega - \nu)t] \tag{56}$$

the output, in terms of gain and phase shift, would be written as

$$\begin{aligned} V_2{}^{-}(t) = \{ & t'_{\omega+\nu}\sin[(\omega + \nu)t + \theta_{\omega+\nu}] \\ & + t'_{\omega-\nu}\sin[(\omega - \nu)t + \theta_{\omega-\nu}]\}. \end{aligned} \tag{57}$$

We can approach the form of (57) by writing (54) and (55) respectively, as

$$\tilde{t}_{\omega+\nu}(\phi) = |\tilde{t}_{\omega+\nu}|\, e^{j\phi_{\omega+\nu}}$$

and

$$\tilde{t}_{\omega-\nu}(\phi) = |\tilde{t}_{\omega-\nu}|\, e^{j\phi_{\omega+\nu}}.$$

The upper sideband is then given by

$$\begin{aligned} &\text{Real Part}\left\{|\tilde{t}_{\omega+\nu}|\, e^{j\omega+\nu}e^{j(\omega+\nu)t}\right\} \\ &\quad = |\tilde{t}_{\omega+\nu}|\cos[(\omega + \nu)t + \phi_{\omega+\nu}] \end{aligned} \tag{58}$$

and the lower sideband by

$$\begin{aligned} &\text{Real part}\left\{|\tilde{t}_{\omega-\nu}|\, e^{j\phi_{\omega-\nu}}e^{j(\omega-\nu)t}\right\} \\ &\quad = |\tilde{t}_{\omega-\nu}|\cos[(\omega - \nu)t + \phi_{\omega-\nu}]. \end{aligned} \tag{59}$$

The amplitudes of (58) and (59) are the same as the corresponding terms in (57), but the trigonometric forms

TABLE III

MATRIX ELEMENT COMBINATION FOR DETERMINING NETWORK RESPONSE

Output \ Input	Carrier in Phase at Terminal 1	Carrier Out of Phase Terminal 1	Carrier in Phase at Terminal 2	Carrier Out of Phase Terminal 2
Transmitted Upper Sideband	$\frac{1}{2}(t\tilde{}_{22} - jt\tilde{}_{12})$	$\frac{1}{2}(t\tilde{}_{11} + jt\tilde{}_{21})$	$\frac{1}{4}(1-j)[t\tilde{}_{33} + t\tilde{}_{34} + j(t\tilde{}_{13} + t\tilde{}_{43})]$	$\frac{1}{4}(1+j)[t\tilde{}_{33} - t\tilde{}_{34} + j(t\tilde{}_{43} - t\tilde{}_{44})]$
Transmitted Lower Sideband	$\frac{1}{2}(t\tilde{}_{22}^* - jt\tilde{}_{12}^*)$	$\frac{1}{2}(t\tilde{}_{11}^* + jt\tilde{}_{21}^*)$	$\frac{1}{4}(1-j)[t\tilde{}_{33}^* + t\tilde{}_{34}^* + j(t\tilde{}_{43}^* + t\tilde{}_{44}^*)]$	$\frac{1}{4}(1+j)[t\tilde{}_{33}^* - t\tilde{}_{34}^* + j(t\tilde{}_{43}^* - t\tilde{}_{44}^*)]$
Reflected Upper Sideband	$\frac{1}{2}(t\tilde{}_{42} - jt\tilde{}_{32})$	$\frac{1}{2}(t\tilde{}_{31} + jt\tilde{}_{41})$	$\frac{1}{4}(1-j)[t\tilde{}_{13} + t\tilde{}_{14} + j(t\tilde{}_{23} + t\tilde{}_{24})]$	$\frac{1}{4}(1+j)[t\tilde{}_{13} - t\tilde{}_{14} + j(t\tilde{}_{23} - t\tilde{}_{24})]$
Reflected Lower Sideband	$\frac{1}{2}(t\tilde{}_{42}^* - jt\tilde{}_{32}^*)$	$\frac{1}{2}(t\tilde{}_{31}^* + jt\tilde{}_{41}^*)$	$\frac{1}{4}(1-j)[t\tilde{}_{13}^* + t\tilde{}_{14}^* + j(t\tilde{}_{23}^* + t\tilde{}_{24}^*)]$	$\frac{1}{4}(1+j)[t\tilde{}_{13}^* - t\tilde{}_{14}^* + j(t\tilde{}_{23}^* - t\tilde{}_{24}^*)]$

differ. We can make the respective terms identical by letting

$$\theta_{\omega\pm\nu} = \phi_{\omega\pm\nu} + \pi/2.$$

Then the relation between $t\tilde{}_{\omega\pm\nu}(\theta)$ and $t\tilde{}_{\omega\pm\nu}(\phi)$ is

$$\begin{aligned} t\tilde{}_{\omega\pm\nu}(\theta) &= \left| t\tilde{}_{\omega\pm\nu} \right| e^{j\theta_{\omega\pm\nu}} \\ &= \left| t\tilde{}_{\omega\pm\nu} \right| e^{j(\phi_{\omega\pm\nu}+\pi/2)} \\ &= e^{j\pi/2} \left| t\tilde{}_{\omega\pm\nu} \right| e^{j\phi_{\omega\pm\nu}} \\ &= jt\tilde{}_{\omega\pm\nu}(\phi). \end{aligned} \tag{60}$$

The quantities $t\tilde{}_{\omega\pm\nu}(\theta)$ and $t\tilde{}_{\omega\pm\nu}(\phi)$ differ only in the definition of the phase angle. However, $t\tilde{}_{\omega\pm\nu}(\theta)$ is chosen so that the argument $\theta_{\omega\pm\nu}$ is the phase shift defined by (57). From (60) we see that the correct phase shifts can be determined from the elements of the scattering matrix if we multiply (54) and (55) by j and take the argument of the resulting complex quantities. The gain is the modulus of these quantities and is, of course, unaffected by multiplication by j.

The reasoning of the preceding paragraphs can be used to express the gain and phase shift in terms of the scattering matrix elements for the various input conditions. These relations are summarized in Table III. For the "in-phase" carrier case treated above, the entries for the upper and lower sidebands of the transmitted output are just (54) and (55) multiplied by j. To determine the gain and phase shift for any particular input-output combination, we take the modulus and phase angle of the corresponding entry in Table III.

VI. Discussion of Results

In the preceding sections we have seen how the phase dependent admittance method and the matrix methods can be used to determine the characteristics of a network. The transmission and reflection properties for a subharmonic signal are summarized in Tables I and II. The form of Table I expresses the output in terms of "in-phase" and "out-of-phase" components while Table II gives the information in terms of a total amplitude and phase shift. The response to a modulated signal can be calculated from Table III.

Subharmonic Properties

As indicated earlier, the network we have been analyzing should exhibit both directionality and phase sensitivity. These properties can be verified by calculating the quantities in Tables I and II for some specific cases. The principal parameter which determines the behavior of the network is $r = \rho\omega C_0 Z_0$, the ratio of negative conductance to the characteristic admittance of the transmission line. Appropriate values for this parameter and for $\omega C_0 Z_0$ (which will be necessary to determining the frequency response) are shown in Table IV. Two presently available diodes are cited, one designed for microwave use, and one intended for low frequencies. The table shows that a reasonable value for $\omega C_0 Z_0$ is of the order of 6. If ρ is chosen as $\rho = 0.22$ (a value substantiated by empirical capacitance versus voltage characteristics), we then see that r is in the vicinity of $r = 1.3$.

Table V shows the numerical values of the quantities in Tables I and II for $\alpha = 1$ (no attenuation) and $r = 4/3$. Since a unit input is assumed, these quantities may be considered as gain factors. We see from the table that the only appreciable transmitted signal occurs for an "in-phase" input at terminal 1. Thus we have demonstrated that the network should be able to select a signal of a particular phase and should provide amplification only in one direction.[10] (These properties have also been observed experimentally in a two-capacitor network at 25 Mc by Allen.[11]) The fairly large reflected components indicate a mismatch for certain input phases. In any application of the network these reflections must be

[10] The gain in the reverse direction is close to unity for both phases. In general we cannot expect a traveling-wave type parametric amplifier to give attenuation in the reverse direction for all phases. If we built an amplifier which would attenuate one phase, there would be another phase which is amplified.

[11] Private communication, August 22, 1958.

TABLE IV
CIRCUIT PARAMETERS FOR AVAILABLE VARIABLE CAPACITORS

Frequency	Diode	C_0 at Operating bias	$\omega C_0 Z_0$ for $Z_0=100\Omega$	r for $\rho=0.22$
10 kMc	Texas Instruments Type XD-503	1.0 pf at 0 v	6.3	1.4
25 Mc	Two Pacific Semiconductors Type V-100 in parallel	170 pf at 1.0 v each diode	5.4	1.2

TABLE V
VOLTAGE RESPONSE OF NETWORK TO UNIT INPUT FOR $r=4/3$, $\alpha=1.0$

Output \ Input	In-Phase at Terminal 1	Out-of-Phase at Terminal 1	In-Phase at Terminal 2	Out-of-Phase at Terminal 2
Transmitted in-Phase	5.5	−0.88	−0 88	1.1
Transmitted Out-of-Phase	0.88	0.22	−1.1	−0.88
Total Trans. Amplitude	5.6	0.91	1 4	1.4
Reflected In-Phase	0.24	−0.44	0.24	2.2
Reflected Out-of-Phase	−2.2	−0.05	0.44	−0.05
Total Ref'td. Amplitude	2.2	0.44	0.50	2.2

carefully considered since they can lead to instability in the over-all circuit. It is possible that mismatch can be reduced by such circuit modifications as slightly changing the length of the one-eighth wavelength section of line between the two capacitors or making this section of different characteristic impedance than the input and output lines. The mathematical methods of this paper should provide a powerful tool for analyzing such modifications.

Our matrix treatment has been set up to take account of attenuation between the two variable capacitors. The effect of this attenuation on an "in-phase" input signal is shown in Fig. 7. There the transmitted and reflected signals (expressed in db relative to the input) are plotted as functions of transmission factor (reciprocal attenuation). We see that the transmitted component initially increases to a maximum at $\alpha=0.86$, and then drops off as the attenuation is increased. In terms of the phase dependent admittance analysis, this effect is explained by noting that the attenuation at first reduces the feedback and thus increases the amplification. However, as the attenuation becomes too large, the loss of transmitted signal becomes more important than the gain increase resulting from further reduction in feedback and the output begins to drop. We note also that the attenuation effects a slight reduction in the reflected component.

Fig. 8 shows directionality and phase discrimination ratio as a function of attenuation. These parameters characterize two significant properties of the network. Directionality is defined as the ratio of transmitted output when the signal is incident on terminal 1 to the transmitted power output when the signal is incident on terminal 2. The phase discrimination ratio is the ratio of the transmitted output for an "in-phase" input to the transmitted output for an "out-of-phase" input. The phase discrimination for a signal traveling from terminal 1 to 2 and the directionality for an "in-phase" input are both improved by attenuation.

Frequency Response

In Section V we saw how the complex hypercomplex formalism could be applied to determine the frequency response of the network. The complex hypercomplex analysis was set up to handle an amplitude modulated subharmonic carrier so that the input could be considered as an upper and lower sideband centered about the subharmonic frequency. In this way the problem of considering the idler frequency separately was avoided. Table III gives $t^{\sim}_{\omega\pm\nu}$, the sidebands of the output for an input consisting of equal upper and lower sidebands in terms of scattering matrix elements.

The special form of the input requires some care in describing the bandwidth properties of the network. The input was assumed to be of the form [see (46)]

$$V_{\text{input}} = \sin \omega t \cos \nu t \tag{61}$$

where ω is the subharmonic frequency. A reasonable criterion for the performance of the network is then how well the output as a function of modulation frequency ν conforms to the input. For the purpose of computation, the output was written (57) as

$$V_{\text{output}} = |t^{\sim}_{\omega+\nu}| \sin [(\omega+\nu)t + \theta_{\omega+\nu}] + |t^{\sim}_{\omega-\nu}| \sin [(\omega-\nu)t + \theta_{\omega-\nu}] \tag{62}$$

where $|t^{\sim}_{\omega\pm\nu}|$ and $\theta_{\omega\pm\nu}$ are determined by Table III and (60). Since the output in general does not have equal upper and lower sidebands, (62) represents a distortion of the input. If we assume an antisymmetric phase shift characteristic (substantiated by the numerical results presented in Fig. 10 below) of the form

$$\theta_{\omega\pm\nu} = \theta_0 + \psi(\pm\nu)$$

where

$$\psi(-\nu) = -\psi(\nu)$$

then (62) can be rewritten as

$$V_{\text{output}} = [|t^{\sim}_{\omega+\nu}| + |t^{\sim}_{\omega-\nu}|] \sin [\omega t + \theta_0] \cdot \cos [\nu t + \psi(\nu)] + [|t^{\sim}_{\omega+\nu}| - |t^{\sim}_{\omega-\nu}|] \cos [\omega t + \theta_0] \cdot \sin [\nu t + \psi(\nu)]. \tag{63}$$

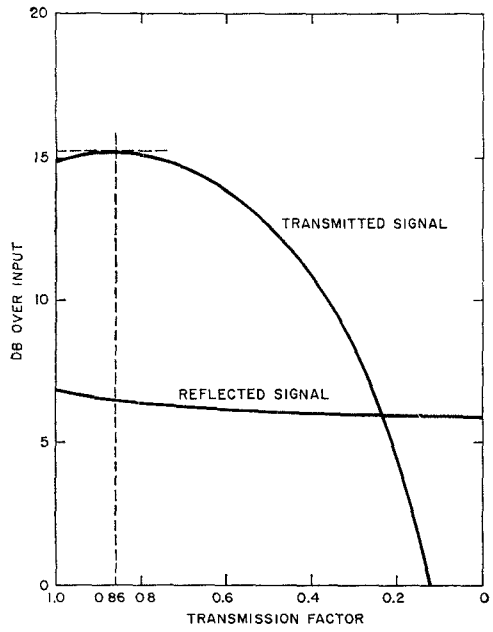

Fig. 7—Transmitted and reflected amplitude vs transmission factor α for "in-phase" input with $r=4/3$.

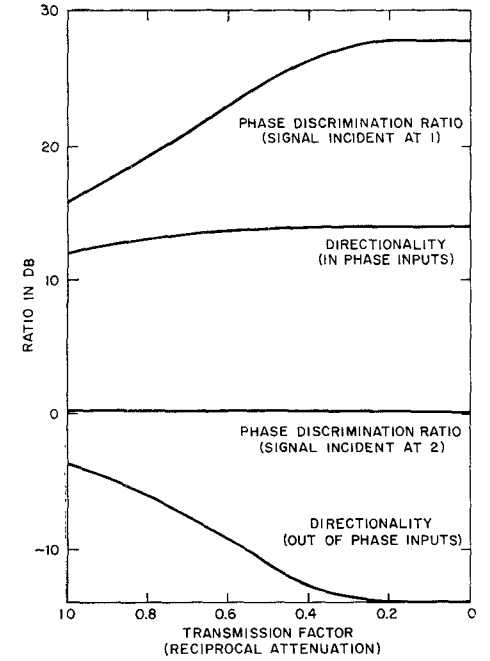

Fig. 8—Directionality and phase discrimination ratio vs transmission factor α for $r=4/3$.

The first term of (63) is of the same form as the input (61) and we may interpret θ_0 as a shift in phase of the carrier and $\psi(\nu)$ as a change in modulation phase. The second term results from the difference in amplitudes of the upper and lower sidebands and, for small difference, can be considered as causing a slight change in the phase angles of the first term.

For the cases we shall discuss θ_0 will be close to $-45°$. Thus the first term of (63) may also be considered as approximating the "in-phase" component of the output carrier. (Note that the input carrier of (61) was "in-phase" with the pump.) The asymmetry between upper and lower sidebands may then be regarded as adding an "out-of-phase" component to the carrier. The interpretation of (63) as an "in-phase" and an "out-of-phase" component is, of course, only an approximation. However, because θ_0 is close to $-45°$, the general features of the frequency response as determined from (63) are the same as would be found if the output were rigorously resolved into "in-phase" and "out-of-phase" carrier components.[12]

The quantities $t\tilde{}_{\omega\pm\nu}$ as a function of modulation frequency have been calculated on an IBM 704 according to Table III and (60) for several values of circuit parameters.[13] Fig. 9 shows a plot of $|t_{\omega\pm\nu}|$ as a function of ν/ω, $|t_{\omega+\nu}|$ being plotted to the right of $\nu=0$ and $|t_{\omega-\nu}|$ being shown on the left. The angles $\theta_{\omega\pm\nu}$ are plotted in similar fashion in Fig. 10. The asymmetry between upper and lower sidebands is evident from Fig. 9. However, the maximum asymmetry within the useful bandwidth is less than 30 per cent for $r=0.6$ and less than 15 per cent for the other cases. Fig. 10 verifies the assumptions we have made about the phase angles. $\theta(\nu=0)$ is seen to differ from $-45°$ by less than $10°$. Figs. 9 and 10 thus substantiate our interpretation of (63) and the fact that the first term gives the predominant behavior. The amplitude of this term (in db relative to the unit input) is plotted in Fig. 11 as a function of modulation frequency. All the curves in Fig. 11 have a constant $\rho=0.222$, but different values of $\omega C_0 Z_0$. This series corresponds to maintaining a constant pump while changing the circuit parameters to vary gain and bandwidth.

In general, bandwidth decreases as the subharmonic gain is increased. We define a modulation bandwidth as the modulation frequency at which the amplitude of the output has dropped by 3 db. Table VI summarizes the gain and bandwidth of these curves. (Since the modu-

[12] By straightforward trigonometry and using the assumed asymmetric form for $\theta_{\omega\pm\nu}$, (63) would be written as

$$V_{\text{out}} = \sqrt{|t\tilde{}_{\omega+\nu}|^2 + |t\tilde{}_{\omega-\nu}|^2 + 2|t\tilde{}_{\omega+\nu}|\,|t\tilde{}_{\omega-\nu}|\cos 2\phi}\cdot\sin(\nu t+\psi+\xi_1)\sin(\omega t-45°) + \sqrt{|t\tilde{}_{\omega+\nu}|^2 + |t\tilde{}_{\omega-\nu}|^2 - 2|t\tilde{}_{\omega+\nu}|\,|t\tilde{}_{\omega-\nu}|\cos 2\phi}\cdot\cos(\nu t+\psi+\xi_2)\cos(\omega t-45°)$$

where

$$\theta_0 = -45° + \phi$$

$$\xi_1 = -\tan^{-1}\left[\frac{|t\tilde{}_{\omega+\nu}| - |t\tilde{}_{\omega-\nu}|}{|t\tilde{}_{\omega+\nu}| + |t\tilde{}_{\omega-\nu}|}\frac{\sin\phi}{\cos\phi}\right]$$

$$\xi_2 = \tan^{-1}\left[\frac{|t\tilde{}_{\omega+\nu}| - |t\tilde{}_{\omega-\nu}|}{|t\tilde{}_{\omega+\nu}| + |t\tilde{}_{\omega+\nu}|}\frac{\cos\phi}{\sin\phi}\right].$$

For $\phi<10°$ and $|t\tilde{}_{\omega+\nu}|-|t\tilde{}_{\omega-\nu}|$ small, this form does not differ appreciably from (63).

[13] We acknowledge the aid of B. Butler, T. C. Chen, Mrs. E. Smith, T. Wilcox, and F. Zarnfaller, who carried out various stages of coding and programming the problem.

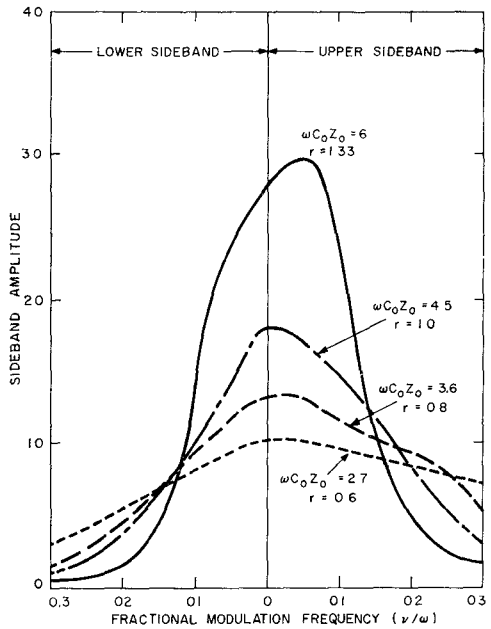

Fig. 9—Sideband amplitude vs fractional modulation frequency for $\rho=0.222$, $\alpha=1.0$.

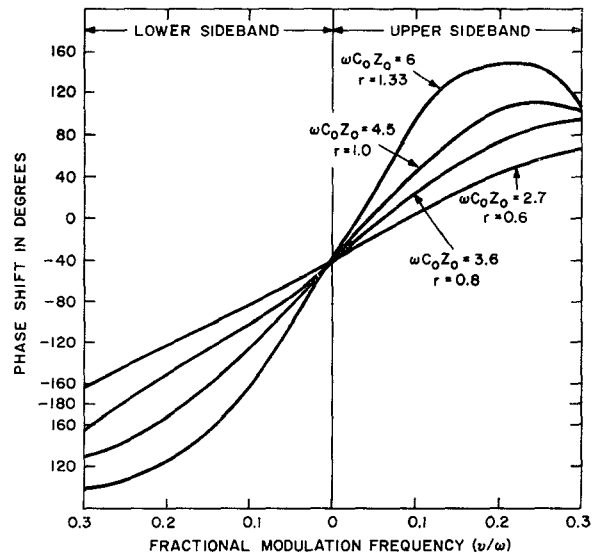

Fig. 10—Phase shifts $\theta_{\omega\pm\nu}$ as a function of fractional modulation frequency for $\rho=0.222$, $\alpha=1.0$.

lation bandwidth has been defined in terms of modulation frequency, we imply that the amplifier passes both the upper and lower sidebands. Therefore, in comparing the properties discussed here with those of amplifiers whose performance is stated in terms of a single input frequency, it would be appropriate to multiply the modulation bandwidths by a factor of two. This factor has been included in Table VI.) An increase in the gain-bandwidth product is noted for the largest value of r. However, $r=1.3$ is close to the maximum value presently achievable, so that actual gain-bandwidth products would not be far outside the range shown in the table. (We should also note that the expressions of Table II indicate a decrease in gain if r were increased beyond about 1.5). The calculations summarized in Table VI thus show that gain can be traded for bandwidth with an essentially constant gain-bandwidth product at moderate values of r. A slight increase in this product is noted for large r. The phase shift within the useful bandwidth is seen from Fig. 10 to be a linear function of ν.

We saw earlier that some attenuation between the variable capacitors slightly improved the subharmonic performance. The effect of this attenuation on the frequency response is shown in Fig. 12 where the responses for $r=4/3$, $\omega C_0Z_0=6$ are shown for several values of attenuation. A predominant feature of these curves is that increasing attenuation decreases the bandwidth. Except for the slight increase in the vicinity of $\alpha=0.86$ (see Fig. 7), attenuation also decreases the gain.

We have now shown how a variable parameter network can be treated using the hypercomplex admittance formalism and how the solutions can be stated in such familiar terms as gain and bandwidth. We proceeded by

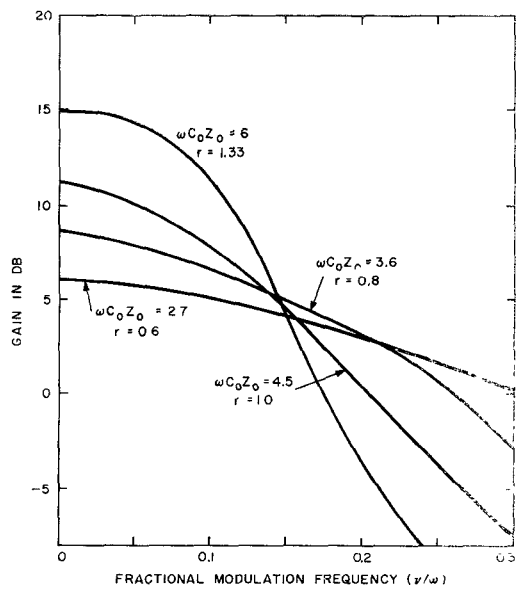

Fig. 11—Gain vs modulation frequency for $\rho=0.222$, $\alpha=1.0$.

TABLE VI

GAIN-BANDWIDTH RELATIONS FOR $\rho=0.222$, $\alpha=1.0$

$r=\rho\omega C_0Z_0$	Gain db	Voltage Gain	Fractional Bandwidth	Voltage Gain×Fract. Bandwidth
0.6	6.0	2.0	0.40	0.80
0.8	8.6	2.7	0.26	0.70
1.0	11.1	3.6	0.20	0.72
1.3	15.0	5.6	0.19	1.06

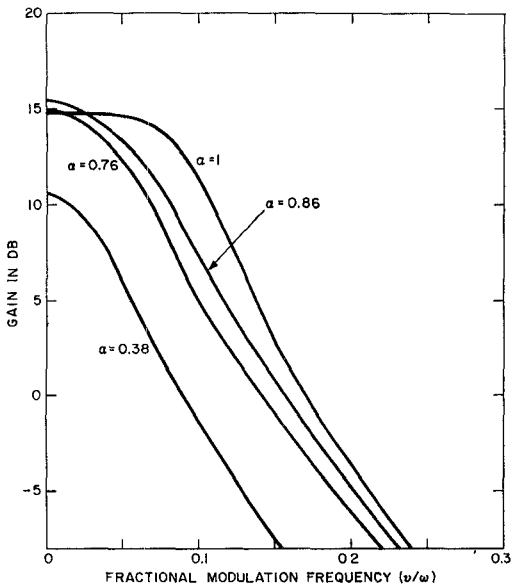

Fig. 12—Network response for several values of transmission factor and $r=1.333$, $\omega CoZo=6$.

first setting up the network problem for constant parameter elements, and then formally substituting the hypercomplex representation for the ordinary admittance functions. In this manner the solution of variable parameter circuits can take advantage of the existing methods of ordinary circuit analysis.

Appendix I
Notation

In general, the notation used throughout this paper is based on the conventional symbols of circuit theory and each term is defined as introduced. However, in our work, voltages and currents are represented by real vectors and by complex vectors, in addition to their usual forms. Impedances and admittances may also be real or complex matrices. To distinguish between the various mathematical forms for these quantities we introduce the following notation:

Vectors (*e.g.*, $\boldsymbol{V}$, $\boldsymbol{I}$): denoted by bold-face.

Matrices (*e.g.*, $\overline{Y}$): denoted by horizontal bar.

Unit matrices of the hypercomplex representation $(1, \hat{\jmath}, \hat{k}, \hat{l})$: denoted by circumflex ($\hat{}$). (Observe that this notation distinguishes between $\jmath=\sqrt{-1}$ and the unit matrix

$$\hat{\jmath}=\begin{pmatrix}0 & -1\\ 1 & 0\end{pmatrix}.$$

Complex quantities (*e.g.*, $\overline{Y}^{\sim}$, $\boldsymbol{V}^{\sim}$): denoted by tilde ($\tilde{}$) next to the symbol.

Acknowledgment

The authors wish to acknowledge many profitable discussions during the course of this work with K. E. Schreiner and M. G. Smith.

Broad-band Directional Couplers*

E. A. MARCATILI†, MEMBER, IRE, AND D. H. RING†, SENIOR MEMBER, IRE

Summary—**It is shown how to connect two identical hybrids to obtain a directional coupler of arbitrary power division that operates over a broader band than that of the components. The broad-banding technique is possible with a certain kind of hybrid that includes Riblet couplers, multihole hybrids, coaxial hybrids and semioptical hybrids, but excludes *T* hybrids and ring hybrids.**

Riblet couplers have a geometry particularly adaptable to the broad-banding technique. Where the balance of one of these couplers is better than 1 db, the balance of the broad-band hybrid can be made better than 0.16 db.

The broad-banding technique is particularly effective in the case of the 100 per cent transfer directional coupler type of circuit used for band separation filters and radar duplexers. In the semioptical waveguide band-splitting filters the bandwidth can be increased from about one to about four octaves (35–75 kMc to 35–580 kMc).

* Received December 11, 1961; revised manuscript received February 16, 1962.

† Bell Telephone Laboratories, Holmdel, N. J.

Introduction

IN A LARGE VARIETY of directional couplers such as the Riblet coupler,[1] the multihole directional coupler,[2] the coaxial directional coupler[3] and the semioptical directional coupler,[4] the power division varies with frequency. We show here that it is possible to connect two identical hybrids[5] in such a way that the

[1] H. J. Riblet, "The short-slot hybrid junction," PROC. IRE, vol. 40, pp. 180–184; February, 1952.

[2] S. E. Miller, "Coupled wave theory and waveguide applications," *Bell Sys. Tech. J.*, vol. 33, pp. 661–719; May, 1954.

[3] E. A. Marcatili, "A circular electric hybrid junction and some channel-dropping filters," *Bell Sys. Tech. J.*, vol. 40, pp. 185–196; January, 1961.

[4] E. A. Marcatili and D. L. Bisbee, "Band-splitting filter," *Bell Sys. Tech. J.*, vol. 40, pp. 197–212; January, 1961.

[5] As usual we understand the hybrid to be a directional coupler with 50–50 power division at least at one frequency of the band of operation.